Motion Estimation of Common Carotid Artery Wall Using a H_∞ Filter Based Block Matching Method

Zhifan Gao[1,2,3], Huahua Xiong[4], Heye Zhang[1,3], Dan Wu[1,2,3], Minhua Lu[5], Wanqing Wu[1,3], Kelvin K.L. Wong[6], and Yuan-Ting Zhang[1,3,7]

[1] Shenzhen Institutes of Advanced Technology, Chinese Academy of Sciences, China
[2] Shenzhen College of Advanced Technology, University of Chinese Academy of Sciences, China
[3] Key Lab for Health Informatics of Chinese Academy of Sciences, China
[4] Department of Ultrasound, The Second People's Hospital of Shenzhen, China
[5] Department of Biomedical Engineering, School of Medicine, Shenzhen University, China
[6] School of Computer Science and Software Engineering, University of Western Australia, Australia
[7] The Joint Research Centre for Biomedical Engineering, Department of Electronic Engineering, Chinese University of Hong Kong, China

Abstract. The movement of the common carotid artery (CCA) vessel wall has been well accepted as one important indicator of atherosclerosis, but it is still one challenge to estimate the motion of vessel wall from ultrasound images. In this paper, a robust H_∞ filter was incorporated with block matching (BM) method to estimate the motion of carotid arterial wall. The performance of our method was compared with the standard BM method, Kalman filter, and manual traced method respectively on carotid artery ultrasound images from 50 subjects. Our results showed that the proposed method has a small estimation error (96 μm for the longitudinal motion and 46 μm for the radial motion), and good agreement (94.03% results fall within 95% confidence interval for the longitudinal motion and 95.53% for the radial motion) with the manual traced method. These results demonstrated the effectiveness of our method in the motion estimation of carotid wall in ultrasound images.

Keywords: vessel wall motion, carotid ultrasound, H_∞ filter, block matching.

1 Introduction

Stiffness of carotid artery has been considered as an important risk marker of severe atherosclerosis [1], which is the main cause of morbidity and mortality related to cardiovascular diseases. A number of studies have attempted to characterize the arterial stiffness from the motion of carotid artery [2]. In particular, the longitudinal motion of carotid wall have recently been recognized in an Editorial

N. Navab et al. (Eds.): MICCAI 2015, Part III, LNCS 9351, pp. 443–450, 2015.
DOI: 10.1007/978-3-319-24574-4_53

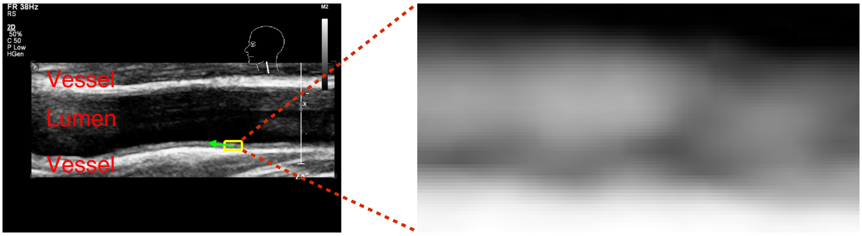

Fig. 1. Example of the ultrasound image of the CCA. The enlarged region (right), corresponding to the yellow rectangle (left), represents the ROI for tracking the motion of carotid vessel. The green arrow is the displacement vector of ROI.

in American Journal of Physiology for its potential importance for the development process of atherosclerosis and recognized at the Royal Swedish Academy of Engineering Sciences annual meeting 2012 [3,4]. Most of these attempts utilized the block matching (BM) method to estimate radial and longitudinal tissue motion of carotid artery from ultrasound image sequences [5]. There are four important issues in the BM method: 1) the size of reference block, 2) the searching range, 3) the distortion function, and 4) the estimation strategy.

The size of reference block always plays an important role in BM method [6]. The influence from the size of reference block on the motion estimation of carotid artery was investigated in [5] by comparing longitudinal and radial displacements generated by different reference blocks. The searching range is another factor to determine the accuracy of BM method. However, the large search range would lead to high computation cost. The tradeoff between the computational cost and the accuracy has been carefully evaluated in the motion estimation from the ultrasound image of carotid artery [7]. The distortion function is used to measure the similarity between the reference block and the candidate block [8], and the cross correlation is one frequently used distortion function in the motion tracking of carotid artery [9]. However, the cross correlation can be easily influenced by the time-variant speckle noise in the ultrasound images. Therefore, normalized cross correlation was proposed to compress the speckle noise in the motion estimation in carotid artery ultrasound images [5]. The estimation strategy is to determine the location of the block from frame to frame in the ultrasound image sequences. Most recent works adopted the adaptive schemes, such as the Kalman filter [2] and the Hilbert transform [10], for estimating the motion of carotid artery. The main problem of Kalman filter is under the Gaussian statistics assumptions. However, uncertainties, such as image noise, sparse image data, and model uncertainty often encountered in practical cases might not be Gaussian statistics. Furthermore, the Kalman filter always performs well only if the filter parameters are reasonably set. In practice, it is very difficult to obtain proper filter parameters because of complexity of the problem. Thus, the issue of robust estimation becomes paramountly important.

In this paper, we introduce a modified BM method using the H_∞ filter to estimate longitudinal and radial motion of CCA. This algorithm differs from the

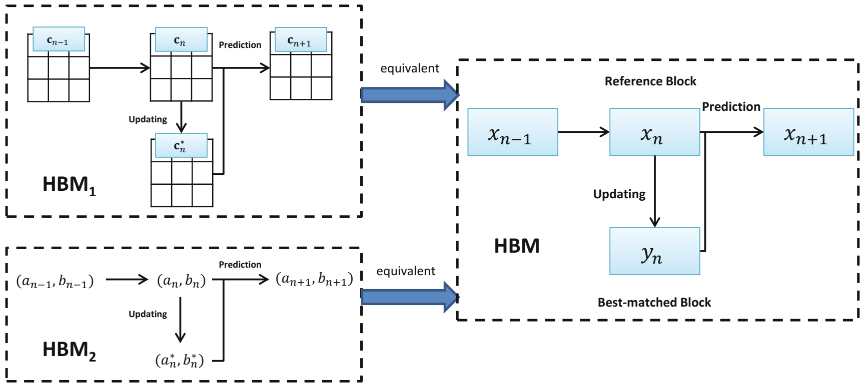

Fig. 2. The flowcharts of HBM$_1$ and HBM$_2$, that can be generalized to the same flowcharts HBM.

previous Kalman approach mainly in the following two aspects: 1) no a priori knowledge of noise statistics is required; and 2) the worst possible effects of the image noises can be minimized because H_∞ filter is a minimax estimator [11], which will ensure that if the disturbances are small, the estimation errors will be as small as possible [12,13]. The performance of our method is evaluated using a set of 50 ultrasound image sequences from 50 subjects by comparing to the manual traced results by one ultrasound physician and three other methods: standard BM method (BM), Kalman-based BM (KBM), update of BM's estimation applying Kalman filter during tracking (KDBM).

2 Methodology

The proposed H_∞-based Block Matching (HBM) for motion estimation of carotid vessel from frame to frame can be divided into two steps: 1) prediction step and 2) updating step. In the prediction step, the best-matched block $\mathcal{B}_{best}$ is estimated from the reference block $\mathcal{B}_{ref}$ in the same frame. In the updating step, the reference block $\mathcal{B}'_{ref}$ in the next frame is estimated from $\mathcal{B}_{best}$ in the current frame. Before HBM, the ultrasound sequence should be preprocessed as follows: 1) inhomogeneity of intensity distributions across frames can influence the subsequent block matching method. It leads to the different dynamic ranges in frames, and moreover makes the same tissues in frames have different range of the pixel value. Thus, every frame in the ultrasound sequence should be normalized into [0, 255] [14]. It can also improve the image quality by changing image contrast; 2) considering the tradeoff between the tracking accuracy and the computational cost, the ultrasound sequence is spatially interpolated using the bilinear method for tracking the sub-pixel motion of carotid artery, which magnifies the image by 3 times and 3) an user-defined reference block (ROI) on the carotid arterial wall in the first frame of the ultrasound sequence is selected with size 0.36 mm $\times$ 0.18 mm. And then the search range can be located, which

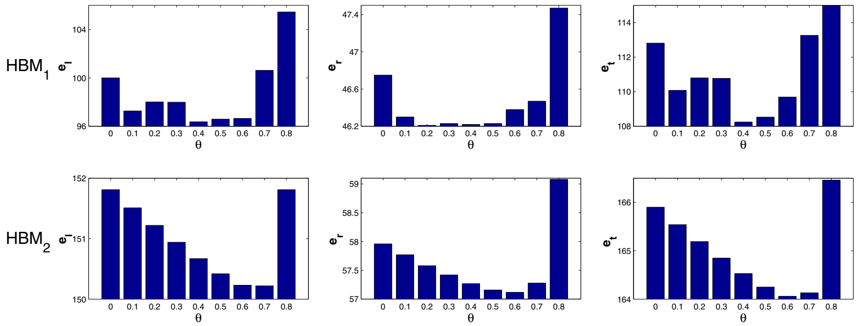

Fig. 3. The mean error of the longitudinal (e_l), radial (e_r) and total displacement (e_t) in μm of the proposed method (HBM_1 in the top row and HBM_2 in the bottom row).

is a rectangle region with size 1.08 mm × 0.36 mm, and its center is same with its corresponding ROI. Figure 1 shows the example of ROI.

Prediction Step. In the prediction step, the reference block $\mathcal{B}'_{ref}$ in the next frame is estimated from the reference block $\mathcal{B}_{ref}$ and the best-matched block $\mathcal{B}_{best}$ in the current frame by H_∞ filter. H_∞ filter can generate the best estimate of the state of a dynamic system by minimizing the worst-case estimation error, and the variation of the reference block $\mathcal{B}_{ref}$ can be modeled as a time-invariant discrete dynamic system:

$$\begin{aligned} \mathbf{x}_{n+1} &= \mathbf{x}_n + \mathbf{w}_n, \\ \mathbf{y}_n &= \mathbf{x}_n + \mathbf{v}_n, \\ \mathbf{z}_n &= \mathbf{x}_n, \end{aligned} \tag{1}$$

where n is the frame index, $\mathbf{w}_n$ and $\mathbf{v}_n$ are noise terms, $\mathbf{x}_n$ and $\mathbf{y}_n$ are matrices corresponding to the reference block $\mathcal{B}_{ref}$ and the best-matched block $\mathcal{B}_{best}$. $\mathbf{x}_{n+1}$ corresponds to the reference block $\mathcal{B}'_{ref}$ in the next frame.

In order to find an optimal estimate $\hat{\mathbf{z}}_n$ of $\mathbf{z}_n$, we need to minimize the cost function J [11], Because the direct minimization of J is not tractable, a strategy for generating the best estimation of $\hat{\mathbf{x}}_{n+1}$ is developed by making the cost function J satisfying an upper bound. Let θ be the reciprocal of the upper bound. This strategy can be formulated as follows [11]:

$$\begin{aligned} \mathbf{K}_n &= \mathbf{P}_n[\mathbf{I} - \theta\mathbf{S}_n\mathbf{P}_n + \mathbf{R}_n^{-1}\mathbf{P}_n]^{-1}\mathbf{R}_n^{-1}, \\ \mathbf{P}_{n+1} &= \mathbf{P}_n[\mathbf{I} - \theta\mathbf{S}_n\mathbf{P}_n + \mathbf{R}_n^{-1}\mathbf{P}_n]^{-1} + \mathbf{Q}_n, \\ \hat{\mathbf{x}}_{n+1} &= \hat{\mathbf{x}}_n + \mathbf{K}_n(\mathbf{y}_n - \hat{\mathbf{x}}_n), \end{aligned} \tag{2}$$

where $\mathbf{Q}_n$ and $\mathbf{R}_n$ are the covariance matrices of the noise terms $\mathbf{w}_n$ and $\mathbf{v}_n$ respectively, $\mathbf{S}_n$ is the user-specified symmetric positive definite matrix, $\mathbf{P}_n$ is the covariance of the estimation error in the frame index n, and $\mathbf{I}$ is the identity matrix. In our method, we set $\mathbf{Q}_n = \mathbf{R}_n = \mathbf{S}_n = \mathbf{I}$, and $\mathbf{x}_1$ corresponds to the ROI selected in the first frame. In addition, in order to obtain the steady-state solution of Equation (2), we set $\mathbf{P}_{n+1} = \mathbf{P}_n$ and $\mathbf{K}_{n+1} = \mathbf{K}_n$.

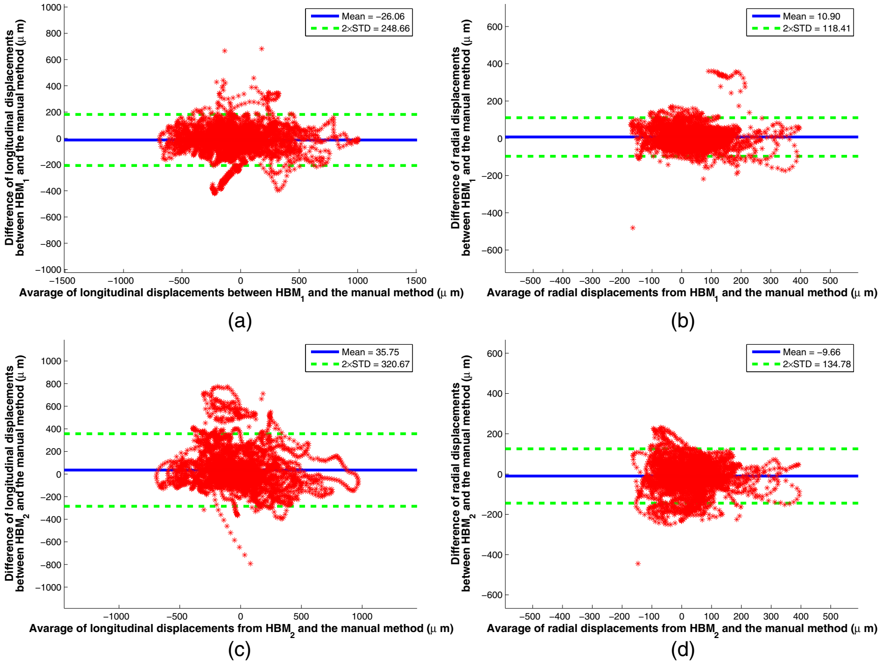

Fig. 4. The Bland-Altman analysis between HBM and manual method. (a) and (b) represent the longitudinal displacements and radial displacements for HBM1 respectively. (c) and (d) represent the longitudinal displacements and radial displacements for HBM2 respectively.

Updating Step. In the updating step, the best-matched block $\mathcal{B}_{best}$ is estimated from the reference block $\mathcal{B}_{ref}$ by the block matching method with normalized cross correlation [5].

Two Implementations. We execute the HBM through two indenpendent implementations: HBM_1 and HBM_2. In HBM_1, $\mathbf{x}_n$ is the vector of the pixel intensity $\mathbf{c}_n$ in the reference block $\mathcal{B}_{ref}$, that is for $\forall i \in \{1, 2, ..., M\}$, the value of the ith element in $\mathbf{x}_n$ equals to the gray value of the ith pixel in the reference block, and M is number of elements in $\mathbf{x}_n$. Similarly, $\mathbf{y}_n$ is the vector of pixel intensity $\mathbf{c}_n^*$ in the best-matched block $\mathcal{B}_{best}$, computed from $\mathcal{B}_{ref}$ by the block matching algorithm. Then, the pixel intensity $\mathbf{c}_{n+1}$ of the reference block $\mathcal{B}'_{ref}$ in the next frame is estimated by $\mathbf{x}_n$ and $\mathbf{y}_n$ using Equation (2). In HBM_2, $\mathbf{x}_n$ is the center location of the reference block $\mathcal{B}_{ref}$, that is $\mathbf{x}_n = (a_n, b_n)$, where a_n and b_n are x-coordinate value and y-coordinate value, respectively. Similarly, $\mathbf{y}_n$ is the center location (a_n^*, b_n^*) of the best-matched block $\mathcal{B}_{best}$, computed from $\mathcal{B}_{ref}$ by the block matching algorithm. Then the center location (a_{n+1}, b_{n+1}) of the reference block $\mathcal{B}'_{ref}$ in the next frame is estimated by $\mathbf{x}_n$ and $\mathbf{y}_n$ using Equation (2). Figure 2 illustrates the flowcharts of HBM1 and HBM2 and shows that the two flowcharts are equivalent.

Table 1. The comparison between BM, KBM, KDBM, $HBM_1(\theta=0.4)$ and $HBM_2(\theta=0.6)$ in μm.

Error	BM	KBM	KDBM	HBM_1	HBM_2
e_l	150.42±148.24	100.00±100.37	151.81±147.18	96.37±85.93	150.22±148.86
e_r	57.16±39.83	50.76±41.52	57.96±39.46	46.22±38.26	57.12±39.92
e_t	164.25±149.83	112.81±106.08	165.91±148.57	109.25±91.24	164.06±150.13

3 Results

One ultrasound physician with more than 10-year experiences collected all the ultrasound data on CCA using a high-resolution ultrasound system (iU22, Philips Ultrasound, Bothell, WA, USA) and a 7.5MHz liner array transducer. All the imaging data then were saved as DICOM format into CDs for off-line analysis. During the collection, the subjects were supine in the bed, with the head turned 45° away from the examined side. In the end, a total of 50 ultrasound image sequences from 50 subjects are used in this study. The study protocol was designed according to the principles of the Declaration of Helsinki and then approved by the Ethics Committee of the Second People's Hospital of Shenzhen in China. Each participant was informed of the purpose and procedure of this study. Informed consent was obtained from each participant. We implement all the codes using Matlab R2012a on a desktop computer with Intel(R) Xeon(R) CPU E5-2650(2.00 GHz) and 32GB DDR2 memory. In the experiments, the motion of carotid artery estimated by our method were compared to the manual traced results by the same ultrasound physician, which is considered as the ground truth.

In order to evaluate the performance of our method quantitatively, we calculated the radial displacement D_r and the longitudinal displacement D_l with respect to the first frame in the ultrasound image sequence. Then the longitudinal error e_l and the radial error e_r of the displacement were computed to analyze the difference between our method and manual traced results,

$$e_l = \sqrt{\frac{1}{N}\sum_{n=1}^{N}(D_l^m(n) - D_l^h(n))^2}, \quad e_r = \sqrt{\frac{1}{N}\sum_{n=1}^{N}(D_r^m(n) - D_r^h(n))^2}, \tag{3}$$

where $D_l^m(n)$ and $D_r^m(n)$ are measured by manual, $D_l^h(n)$ and $D_r^h(n)$ are estimated by our method. Then the total error can be computed by $e_t = \sqrt{e_l^2 + e_r^2}$. Through e_l, e_r and e_t, we can determine the value of θ. In Figure 3, we can see that the $\theta = 0.4$ is better than other values of θ in HBM_1. Similarly, $\theta = 0.6$ in HBM_2 is better than other values. Moreover, HBM_1 is better than HBM_2 because all the minimum errors in HBM_1 are less than those in HBM_2. Additionally, we used the Bland-Altman method to analyze the agreement between our method and the manual method. As seen in Figure 4. For the longitudinal displacement and the radial displacement in HBM_1, 94.03% and 95.53% of points fall within the 95% confidence interval in the Student t-test, respectively.

In HBM_2, the results are 93.47% and 92.38%. At last, our method was compared with three other methods using manual traced results as ground truth: the standard BM method [5], Kalman-based BM (KBM) [7], update of BM's estimation applying Kalman filter during tracking (KDBM) [7]. Table 1 shows the comparative results of these methods.

4 Discussion and Conclusion

We developed a H_∞ filter based BM method to estimate the motion of carotid artery wall from the ultrasound image sequences. In each imaging frame, we compute the best-matched block by the reference block using the block matching method. Then, the reference block in the next frame can be estimated by the reference block and the best-matched block in the current frame using a H_∞ filter. Additionally, we used two independent strategies (HBM_1 and HBM_2) to implement the proposed method. And the two implementations are based on the pixel intensity and center location of the reference block, respectively. In the experiments, the results generated by our H_∞ filter based BM method with different values of θ were evaluated using 50 ultrasound image sequences and compared to manual traced results by one experienced ultrasound physician. Based on these experiments, the optimal values of θ for HBM_1 ($= 0.4$) and HBM_2 ($= 0.6$) can be obtained according to minimum error shown in Table 1. In addition, we can see that the proposed H_∞ filter with $\theta \geqslant 0.9$ is unstable as the error is significantly in Figure 3. Moreover, our method were also compared to three recent methods using manual traced results as the ground truth: BM, KBM and KDBM. Table 1 shows that the motion trajectory computed by our H_∞ filter based BM method (HBM_1 with $\theta = 0.4$ and HBM_2 with $\theta = 0.6$) are more accurate than three other methods. These experiments can demonstrate the effectiveness of our method in the motion estimation of carotid artery wall from ultrasound image sequences. Using the motion tracking of carotid vessel, we will focus on the investigation of the properties of vessel wall (especially the longitudinal motion) and its relationship with physiological parameters related to cardiovascular disease (such as wall shear strain and pulse wave velocity) in the future.

Acknowledgements. We thank support from the Guang-dong Innovation Research Team Fund for Low-cost Health-care Technologies in China, the Key Lab for Health Informatics of the Chinese Academy of Sciences, the External Cooperation Program of the Chinese Academy of Sciences (GJHZ1212), National Natural Science Foundation of China (No. 61471243) and Shenzhen Innovation Funding (JCYJ20140414170821190).

References

1. Yli-Ollila, H., Laitinen, T., Weckström, M., Laitinen, T.M.: Axial and radial waveforms in common carotid artery: An advanced method for studying arterial elastic

properties in ultrasound imaging. Ultrasound in Medicine & Biology 39(7), 1168–1177 (2013)
2. Zahnd, G., Orkisz, M., Srusclat, A., Moulin, P., Vray, D.: Evaluation of a kalman-based block matching method to assess the bi-dimensional motion of the carotid artery wall in b-mode ultrasound sequences. Medical Image Analysis 17(5) (2013)
3. Cinthio, M., Ahlgren, R., Bergkvist, J., Jansson, T., Persson, W., Lindström, K.: Longitudinal movements and resulting shear strain of the arterial wall. American Journal of Physiology-Heart and Circulatory Physiology 291(1) (2006)
4. Ahlgren, R., Cinthio, M., Steen, S., Nilsson, T., Sjöberg, T., Persson, W., Lindström, K.: Longitudinal displacement and intramural shear strain of the porcine carotid artery undergo profound changes in response to catecholamines. American Journal of Physiology-Heart and Circulatory Physiology 302(5) (2012)
5. Golemati, S., Sassano, A., Lever, M.J., Bharath, A.A., Dhanjil, S., Nicolaides, A.N.: Carotid artery wall motion estimated from b-mode ultrasound using region tracking and block matching. Ultrasound in Medicine & Biology 29, 387–399 (2003)
6. Ramirez, B.: Performance evaluation and recent advances of fast block-matching motion estimation methods for video coding. In: Kropatsch, W.G., Kampel, M., Hanbury, A. (eds.) CAIP 2007. LNCS, vol. 4673, pp. 801–808. Springer, Heidelberg (2007)
7. Gastounioti, A., Golemati, S., Stoitsis, J.S., Nikita, K.S.: Carotid artery wall motion analysis from b-mode ultrasound using adaptive block matching: in silico evaluation and in vivo application. Physics in Medicine and Biology 58(24), 8647–8661 (2013)
8. Metkar, S., Talbar, S.: Motion Estimation Techinques for Digital Video Coding. Springer (2013)
9. Lewis, J.P.: Fast template matching. In: Proceeding of Vision Interface, pp. 120–123 (1995)
10. Zahnd, G., Orkisz, M., Balocco, S., Sérusclat, A., Moulin, P., Vray, D.: A fast 2d tissue motion estimator based on the phase of the intensity enables visualization of the propagation of the longitudinal movement in the carotid artery wall. In: IEEE International Ultrasonics Symposium (IUS), pp. 1761–1764. IEEE (2013)
11. Simon, D.: Optimal State Estimation: Kalman, H_∞ and Nonlinear Approaches. Wiley-Interscience (2006)
12. Hassibi, B., Sayed, A.H., Kailath, T.: H_∞ Optimality of the LMS Algorithm. IEEE Transactions on Signal Processing 44(2) (1996)
13. Liu, H., Wang, S., Fei, G., Tian, Y., Chen, W., Hu, Z., Shi, P.: Robust Framework for PET Image Reconstruction Incorporating System and Measurement Uncertainties. PLOS One 7(3) (2012)
14. Gonzalez, R., Woods, R., Digital Image Processing. Pearson Education (2009)